Korean J. Chem. Eng., 39(3), 475-483 (2022)
DOI: 10.1007/s11814-021-0991-1

pISSN: 0256-1115
eISSN: 1975-7220

REVIEW PAPER

Tailoring physical and chemical microenvironments by polyether-amine in blended membranes for efficient CO_2 separation

Xia Lv*, Xueqin Li*,†, Lu Huang*, Siyuan Ding*, Yin Lv*, and Jinli Zhang*,,†**

*School of Chemistry and Chemical Engineering/Key Laboratory for Green Processing of Chemical Engineering of Xinjiang Bingtuan, Shihezi University, Shihezi, Xinjiang, 832003, China
**Key Laboratory for Green Chemical Technology of Ministry of Education, School of Chemical Engineering and Technology, Tianjin University, Tianjin 300072, China
(*Received 19 June 2021 • Revised 19 October 2021 • Accepted 20 October 2021*)

Abstract−Pebax® MH 1657 (Pebax)-based blend membranes with different polyether-amine (PEA) loadings were designed and fabricated for efficient CO_2 separation. The CO_2 separation performance of Pebax/PEA blend membranes was greatly improved in comparison with that of pure membranes. This was mainly because the introduced PEA tailored the physical and chemical microenvironments in blend membranes. Specifically, PEA was a liquid-like additive, which was beneficial to reduce the mass transfer resistance of gases and increase CO_2 permeability. Meanwhile, PEA contained amino groups that acted as mobile carriers to tailor the chemical microenvironment in blend membranes. The mobile carriers preferentially reacted reversibly with CO_2 molecules, facilitating CO_2 transport in membranes. Compared with CO_2/CH_4 separation performance of pure Pebax membrane, CO_2 permeability and CO_2/CH_4 separation factor of Pebax/PEA-3 increased by 144.8% and 29.4%, respectively. This study suggests that PEA is a promising membrane material for tailoring the physical and chemical microenvironments in blend membranes for efficient CO_2 separation.

Keywords: Pebax, Polyether-amine, Blend Membrane, Microenvironments, CO_2 Separation

INTRODUCTION

As a green and environmentally friendly clean energy source, natural gas consists primarily of methane (CH_4). However, the presence of harmful impurities (CO_2) in natural gas reduces the heat of combustion of CH_4 and causes corrosion problems in gas pipelines, which in turn restricts the compression and transmission of natural gas [1-7]. Thus, CO_2 removal is an essential process in the industrial application of natural gas. Membrane-separation technology has attracted significant attention in the field of CO_2 separation, deriving from its advantages of environmental friendliness, low-energy requirement, and high efficiency [8-11].

CO_2 separation performance of membranes principally depends on the membrane materials, which impact the efficiency of CO_2 separation process [12-15]. Therefore, it is vital to utilize the membrane materials that possess high CO_2 permeability and CO_2/CH_4 selectivity. Polymeric membranes have been widely studied for their good processability, easy fabrication, and low cost. Nevertheless, polymeric membranes are generally restricted by their inherent "trade-off" relationship between permeability and selectivity [4,16,17].

To further improve CO_2 permselectivity, polymeric membranes have been modified by many methods, including blending, cross-linking, and grafting [18-22]. The blending method has attracted significant research attention because it is an easy and simple method to fabricate blend membranes, which consist of polymeric materials and additives [23]. Moreover, the introduced suitable additives can improve both CO_2 permeability and selectivity of blend membranes effectively.

In recent years, blend membranes have been developed by introducing a variety of additives, including polyethylene glycol (PEG), polyethyleneimine (PEI), ionic liquids (ILs), and amino acid salt (AAS) [24-34]. Feng et al. [35] introduced different molecular weights of PEG into Pebax 1074 to fabricate blend membranes. For low-molecular-weight PEG, Pebax 1074/PEG blend membranes achieved higher CO_2 permeability than that of pure membrane. However, CO_2/N_2 selectivity was unchanged. Car et al. [36] fabricated Pebax® MH 1657 (Pebax)/PEG 200 blend membranes and reported the related gas-separation properties. The results exhibited that CO_2 permeability of Pebax/PEG 200 blend membranes was two-times that of pure membranes, while CO_2/CH_4 selectivity remained constant. Reijerkerk et al. [37] fabricated Pebax/poly (dimethyl siloxane) (PDMS)-PEG_{200} blend membranes. The result indicated that CO_2 permeability of Pebax/PDMS-PEG_{200} blend membrane was five-times higher than that of pure membrane, while CO_2/CH_4 selectivity decreased.

All the above-mentioned studies indicated that the introduced additives containing EO units can effectively increase CO_2 permeability of blend membranes; however, they cause a decrease or constant in CO_2/gas selectivity accordingly. Therefore, gas selectivity of blend membranes that are mixed with additives containing EO units must be improved. It is vital to explore and design additive containing EO units that can improve both CO_2 permeability and selectivity of blend membranes.

Polyether-amine (PEA, also known as polypropylene glycol bis

†To whom correspondence should be addressed.
E-mail: lixueqin861003@163.com, zhangjinli@tju.edu.cn

(2-aminopropyl ether)) is a type of additive containing EO units, comprised primarily by a main chain consisting of polyether oxygen (PEO) and the terminal chain of amino groups [38,39]. On one hand, PEA contains the EO units that have a strong affinity with CO_2, which is beneficial for increasing CO_2 permselectivity. On the other hand, the amino groups of PEA serve as CO_2 carriers that can reversibly react with CO_2, facilitating CO_2 transport. Many studies mainly focused on PEA as modifier to modify fillers in composite membranes for CO_2 separation [38-42]. The problem is that the introduction of the amount of PEA in composite membranes is limited, and the functions of PEA itself in membranes are also limited.

To solve this problem, PEA is directly introduced into the membrane matrix by an easy and simple blending method to fabricate blend membranes. It would be a good strategy to introduce PEA into membranes, because PEA itself as a liquid-like additive is beneficial to reduce the mass transfer resistance of gases. Meanwhile, the amino groups of PEA act as mobile carriers and are favorable to facilitate CO_2 transport. It is expected that the introduction of PEA will improve both gas permeability and selectivity of blend membranes.

In this study, PEA itself as a liquid-like additive was directly introduced into Pebax matrix to fabricate blend membranes for efficient CO_2 separation. The physicochemical properties of the as-prepared blend membranes were systematically characterized and analyzed. The effects of the PEA loadings coupled with different feed pressures and operating temperatures on CO_2/CH_4 separation of Pebax/PEA blend membranes were tested and discussed.

EXPERIMENTAL AND METHOD

1. Materials

Prime materials were used in this experiment. Pebax® MH 1657 (Pebax) was purchased from Shanghai Rongtian Chemical Co.; its chemical structure is shown in Fig. 1(a), polyether-amine (PEA, average molecular weight 400) and anhydrous ethanol were purchased from Aladdin, the chemical structure of PEA is shown in Fig. 1(b). Gases (CO_2/CH_4, H_2) were purchased from Shihezi City Acer Gas Co., Ltd., and deionized water was produced by Shihezi University.

2. Preparation of Membranes

The as-prepared membranes were flat sheets in this experiment. Briefly, a 70 wt% (anhydrous ethanol/deionized water=70/30) ethanol solution, as the organic solvent, was mixed with Pebax, and stirred at 80 °C for 2 h until the solution was uniform; thereafter, it was left standing at room temperature to obtain the Pebax solution

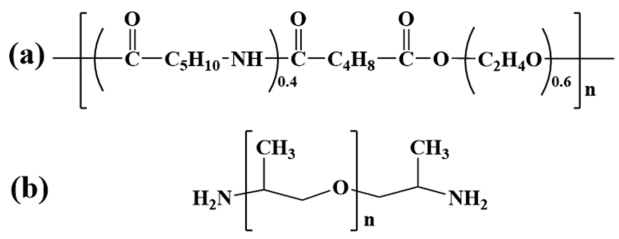

Fig. 1. Chemical structures of (a) Pebax and (b) PEA.

(4.0 wt%). The quantitative PEA was weighted and mixed in the Pebax solution, followed by stirring for 3 h until the solution was uniform, which yielded the solution of blend membranes. The solution was poured into Petri dishes and dried naturally for 48 h. Afterward, the initial membranes were obtained and dried in a vacuum oven for 48 h. Finally, the remaining solvents of membranes were completely removed to obtain the final pure Pebax membrane and blend membranes, and the blend membranes were named Pebax/PEA-*X* (*X* is the mass fraction of PEA). The PEA loadings are defined in Eq. (1):

$$X_{PEA} = \frac{m_{PEA}}{m_{PEA} + m_{Pebax}} \times 100\% \quad (1)$$

where the units of m_{PEA} and m_{Pebax} are g.

3. Characterization of Membranes

Scanning electron microscopy (SEM, JSM-6490 LV) was conducted to observe the morphology of membrane structure. First, membranes were fractured with liquid nitrogen; then, the fractured membranes were coated with metallic gold for approximately 30 s. Fourier transform infrared spectroscopy (FT-IR, BRUKER Vertex 70) was conducted to observe the functional groups and chemical bonds of PEA and blend membranes, defining the chemical structure of blend membranes. Differential scanning calorimetry (DSC, METTLER DSC 1 SF) was conducted to examine the thermal performance of membranes and investigate their glass transition temperature (T_g). Membranes were heated from −75 °C to 250 °C at a heating rate of 10 °C/min. Thermo gravimetric analysis (TGA, STA449F3) was used to determine the thermal behavior of membranes, the testing temperature was in the range of 30-800 °C. X-ray diffraction (XRD, Bruker D8 ADVANCE) analysis was conducted to examine the molecular-chain spacing and the crystalline types of membrane samples in the scan range of 10-90° and at a scan rate of 2°/min. Operation of some characterization items can refer to the literature [43-46]. Tensile force tester (INSTRON 3366) was used to measure the mechanical properties of membranes, and the speed of testing was programmed at 70 mm/min. The membranes should be made into a rectangle with an effective length of 1 cm and width of 0.5 cm. The contact angle was used to investigated the hydrophilicity of membranes, and deionized water was used in this experiment.

4. Gas Permeation Measurement

Based on the conventional constant pressure/variable volume technique, gas separation performance of membranes was investigated using the binary mixture gas system (CO_2/CH_4=20/80 vol%) under a dry condition with the feed gas (CO_2/CH_4) and sweep gas (H_2) fluxes of 50 and 30 mL/min, respectively [47,48]. A schematic diagram and the real picture of self-built permeation measurement equipment are shown in Fig. 2 and Fig. S1 (Supplementary Material), respectively. The as-prepared membranes (12.56 cm^2, central part) were placed into a circular stainless-steel cell to study the gas permeation of membranes. The gas permeation experiments were tested using a temperature range of 25-55 °C and a pressure range of 2-8 bar. The composition of the gases was analyzed using a Shimadzu GC2014C gas chromatograph. All of membranes were measured at least three times to guarantee the reproducibility and reliability of the results.

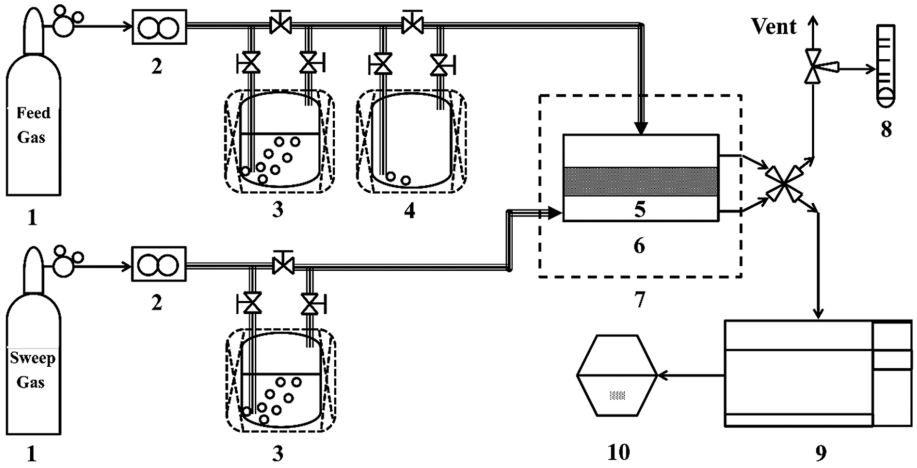

Fig. 2. Schematic diagram of the self-built permeation measurement equipment.

1. Gas cylinder
2. Mass flow meter
3. Humidifier with heating belts
4. Water knockout with heating belts
5. Membrane
6. Permeation cell
7. Oven
8. Soap film flowmeter
9. Gas chromatography
10. Computer

Gas permeation (CO_2 or CH_4) is calculated using Eq. (2):

$$P_i = \frac{Q_i l}{\Delta P_i A} \quad (2)$$

where P_i represents gas (CO_2 or CH_4) permeability (Barrer, 1 Barrer= 10^{-10} cm^3 (STP) cm cm^{-2} s^{-1} $cmHg^{-1}$); Q_i represents the volume velocity in the standard state (cm^3 (STP) s^{-1}); l represents the thickness of membranes; ΔP_i represents the differential pressure on both sides of membranes; and A represents the effective membrane area (cm^2) [49-51].

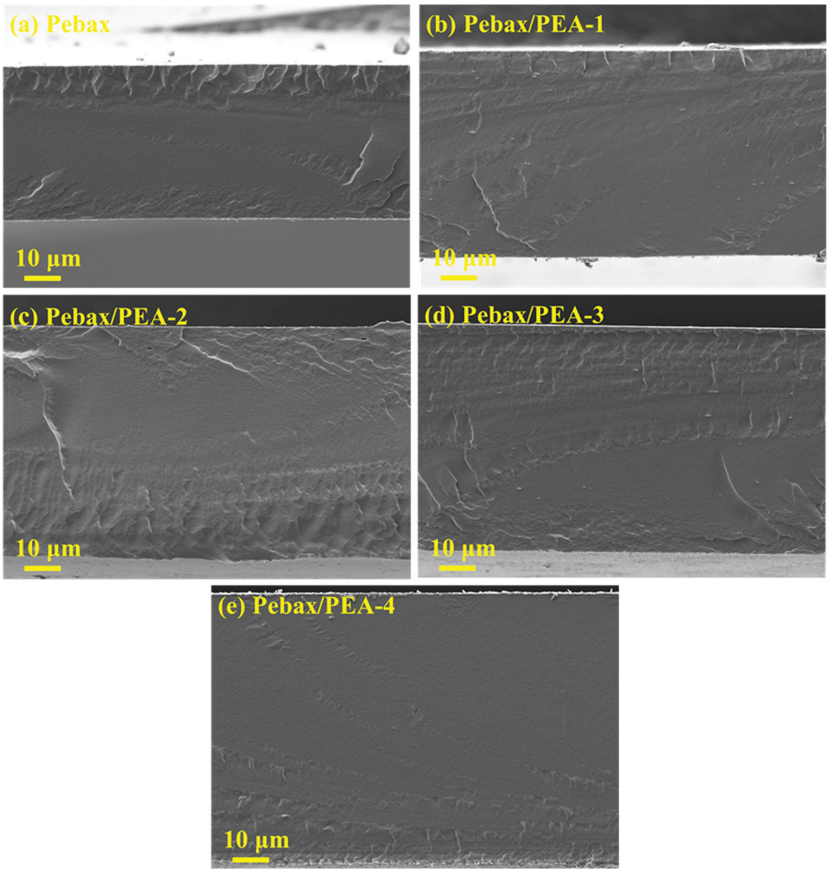

Fig. 3. SEM image of the cross-section of pure Pebax membrane and Pebax/PEA blend membranes: (a) pure Pebax membrane and (b)-(e) Pebax/PEA blend membranes.

Gas selectivity of membranes is expressed by the ratio of the permeability coefficients of component *i* to component *j*, and it is calculated using Eq. (3):

$$\alpha_{ij}=\frac{P_i}{P_j} \quad (3)$$

where if the feedstock gas is a pure gas, α_{ij} is the ideal selectivity of component *i*/*j*, whereas if the feedstock gas is a mixture of gases, α_{ij} is the separation factor of component *i*/*j* [49,52].

RESULTS AND DISCUSSION

1. Characterization of Membranes

1-1. SEM Analysis

The SEM morphologies of pure Pebax membrane and Pebax/PEA blend membranes are presented in Fig. 3. It was observed from Fig. 3(a) that the cross-section of pure Pebax membrane had a homogeneous structure without any defects. The cross-sections of Pebax/PEA blend membranes presented a homogeneous structure. This result indicates that the introduction of PEA had little effect on the cross-sectional morphology of the membrane matrix.

1-2. FT-IR Analysis

The FT-IR spectra of pure Pebax membrane and Pebax/PEA blend membranes are presented in Fig. 4. In the spectrum of pure Pebax membrane, the stretching vibrations of the N-H bond and the H-N-C=O bond are indicated by the infrared characteristic peaks at 3,300 cm^{-1} and 1,640 cm^{-1}, respectively. Conversely, the stretching vibrations of the C=O bond and the C-O-C bond are assigned to the infrared characteristic peaks at 1,732 cm^{-1} and 1,100 cm^{-1}, respectively. The symmetric stretching vibration of the C-H bond is assigned to the infrared characteristic peak at 2,860 cm^{-1}. These results are consistent with the molecular structure formula of Pebax 1657 [6,53]. In the spectrum of PEA, the -NH_2 groups and the stretching vibration of the C-O-C bond are indicated by characteristic infrared peaks at 3,364 cm^{-1} and 1,100 cm^{-1}, respectively.

Fig. 4(a) shows that the bands of blend membranes shifted to high wavenumber in comparison with that of Pebax membrane. It was mainly attributed to the fact that the introduced PEA had amino groups, which can form hydrogen bonding with PA6 chains of Pebax matrix [2]. Meanwhile, no new absorption bands appeared for blend membranes in comparison with that for pure membrane; it implied that there was no chemical interaction between Pebax matrix and PEA.

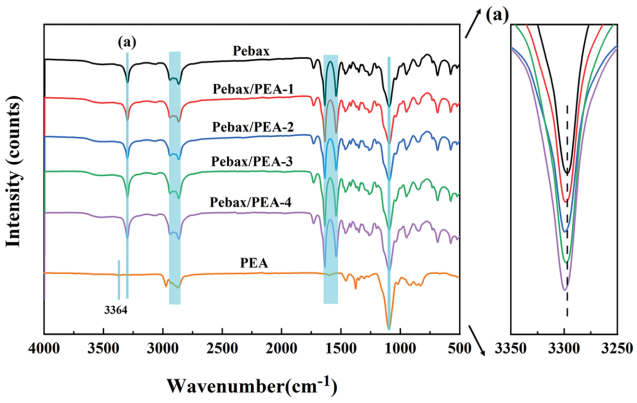

Fig. 4. FT-IR spectra of pure Pebax membrane, Pebax/PEA blend membranes, and PEA: (a) Partial enlarged drawing of membranes.

1-3. Thermal Analysis

The thermal properties and T_g of pure membrane, Pebax/PEA blend membranes were investigated by TGA and DSC, and the corresponding results are exhibited by Fig. 5 and Fig. 6, respectively. The TGA curves of membranes and PEA are shown in Fig. 5. The weight loss of all membranes showed a slight change within the temperature of 100 °C; it was mainly attributed to the evaporation of water molecules [48,54]. The decomposition of PEA occurred at approximately 150 °C. The rapid weight loss occurred around 350 °C for all membranes due to the thermal degradation of Pebax matrix. The results indicate that both blend membranes and pure membrane had a good thermal stability.

Fig. 6 shows DSC curves of pure Pebax membrane, Pebax/PEA blend membranes. Evidently, the T_g of pure Pebax membrane showed at −51.5 °C, which was consistent with the reports [18,53]. The T_g

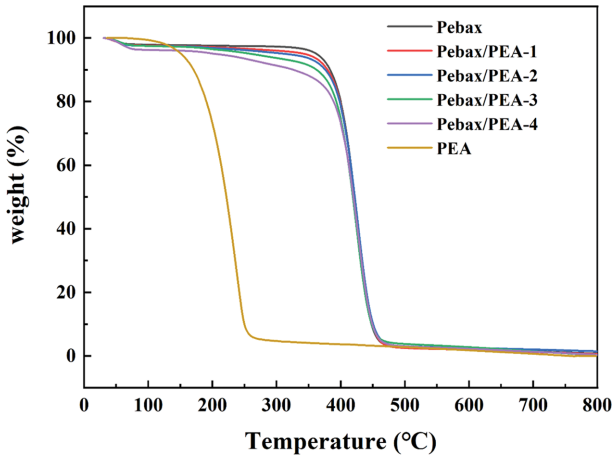

Fig. 5. TGA curves of pure membrane, Pebax/PEA blend membranes and PEA.

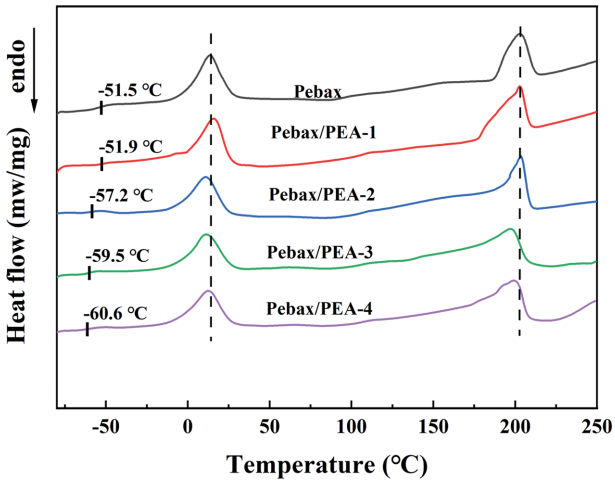

Fig. 6. DSC curves of pure Pebax membrane, Pebax/PEA blend membranes.

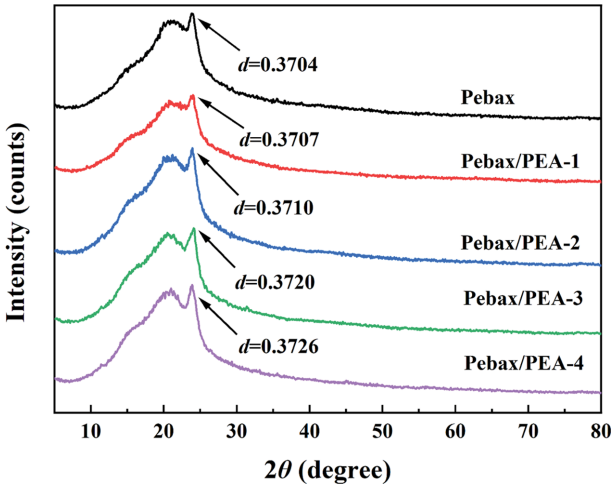

Fig. 7. XRD patterns of pure Pebax membrane and Pebax/PEA blend membranes.

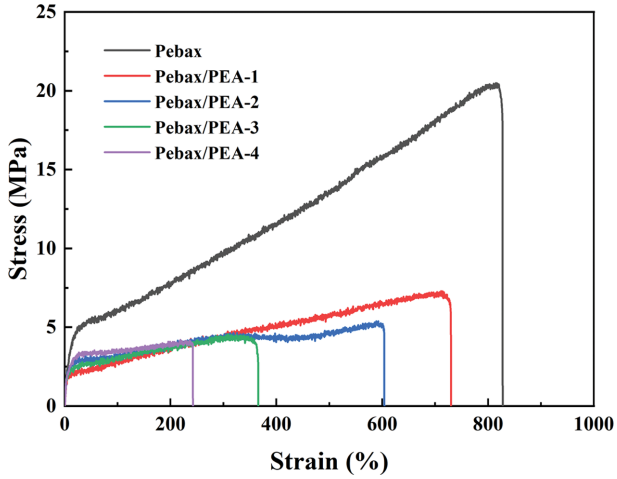

Fig. 8. Stress-strain curves of pure Pebax membrane and Pebax/PEA blend membranes.

values of Pebax/PEA blend membranes continuously declined with increasing PEA loadings. This suggests that Pebax matrix chains became more flexible due to the high chain mobility of PEA with low-molecular-weight [31,35]. Moreover, the decrease in the melting points of PEO and PA also suggests that the introduced PEA increased the flexibility of Pebax matrix chains.

1-4. XRD Analysis

The crystal structure and molecular-chain spacing of the membranes were investigated by XRD, and the corresponding patterns are shown in Fig. 7. It was observed that the strong and broad characteristic diffraction peaks ranging from 15-30 were consistent with the integration of the crystalline and amorphous phases from PA and PEO [6,55]. According to Bragg's law, the average *d*-spacings of pure Pebax membrane and Pebax/PEA blend membranes were calculated [56,57]. Fig. 7 shows that the *d*-spacings of membranes increased from 0.3704 to 0.3726 with increasing PEA loadings; the *d*-spacing values of blend membrane was slightly changed in comparison with that of pure membrane. It means that the introduced PEA had little effect on the physical structure of Pebax polymer.

1-5. Mechanical Property Analysis

The mechanical properties of pure Pebax membrane and Pebax/PEA blend membranes were measured by the tensile force tester, and the corresponding results are shown in Fig. 8 and Table 1. It can be observed from Fig. 8 and Table 1 that the Young's modulus of blend membranes increased with the increase of PEA loadings. It was mainly attributed to the introduced PEA containing amino groups, which strengthened the hydrogen bond interactions with polymer matrix. The elongation at break and tensile strength of blend membranes decreased with increasing PEA loadings, and it resulted because there was no chemical interaction between polymer matrix and additive [40].

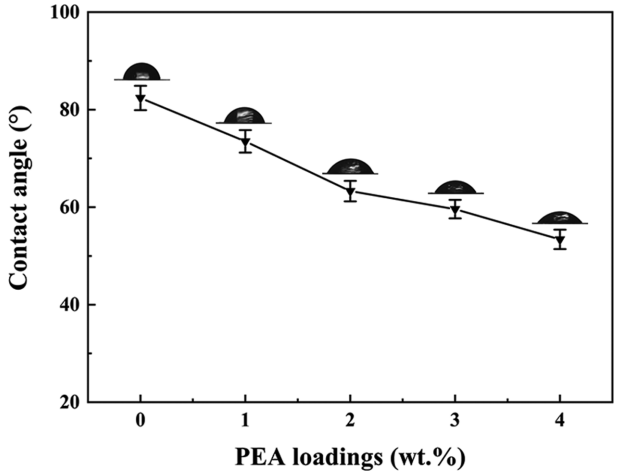

Fig. 9. Relation diagram of the contact angle of pure Pebax membrane and Pebax/PEA blend membranes.

1-6. Contact Angle Analysis

A contact angle experiment was conducted to evaluate the hydrophilicity of pure Pebax membrane and Pebax/PEA blend membranes. The hydrophilicity decreased with an increase in the contact

Table 1. Mechanical properties of pure Pebax membrane and Pebax/PEA blend membranes

Membrane	Elongation at break (%)	Tensile strength (MPa)	Young's modulus (MPa)
Pebax	836.99±22.6	20.49±0.7	24.95±1.3
Pebax/PEA-1	734.49±18.9	7.30±1.3	49.43±1.2
Pebax/PEA-2	609.42±22.4	5.39±2.5	59.15±2.1
Pebax/PEA-3	377.39±24.8	4.57±1.4	67.92±2.5
Pebax/PEA-4	274.40±33.7	4.20±2.1	71.53±1.6

angle, and the experimental results are indicated in Fig. 9. The real contact angle pictures from the camera are shown in Fig. S2 (Supplementary Material). It can be observed that the contact angle of pure Pebax membrane was 82.4±2.5°. The contact angle of the Pebax/PEA blend membranes continuously decreased as the PEA loadings increased in comparison with pure Pebax membrane case. This implies that the introduced PEA improved the hydrophilicity of Pebax/PEA blend membranes. The results are mainly attributed to the hydrophilic PEA with a low molecular weight that was introduced into Pebax matrix.

2. Gas Separation Performance

2-1. Mixed Gas

Fig. 10 exhibits gas permeability and selectivity of pure Pebax membrane and Pebax/PEA blend membranes; the whole experiment was carried out under dry condition, and the operating pressure and temperature were 2 bar and 25 °C, respectively. It can be observed that CO_2 permeability and CO_2/CH_4 separation factor of pure Pebax membrane were 80±1.2 and 18±1.8, respectively. The optimal CO_2/CH_4 separation performance of blend membranes was by Pebax/PEA-3. Correspondingly, CO_2 permeability and CO_2/CH_4 separation factor of Pebax/PEA-3 blend membrane were 195.8± 2.1 Barrer and 23.3±0.3, respectively. This suggests that CO_2 permeability and CO_2/CH_4 separation factor of Pebax/PEA-3 blend membrane increased by 144.8% and 29.4% in comparison with that of pure Pebax membrane, respectively.

Furthermore, CO_2 permeability and CO_2/CH_4 separation factor of Pebax/PEA blend membranes first increased and then decreased with increasing PEA loading. Pebax is a typical solubility-selective membrane material originating from the strong affinity of PEO units to the quadrupolar CO_2 molecules [2,58]. Based on the solution-diffusion mechanism, the main reasons for the increased CO_2 separation performance were as follows: PEA is a liquid-like additive which reduces the mass transfer resistance of gases. The introduced PEA reduces the T_g of the membranes; it is beneficial to increase the flexibility of the polymer chains. Thus, the introduction of liquid-like PEA additive can increase CO_2 diffusivity to promote CO_2 permeation. Moreover, the PEO units of PEA have a strong affinity for CO_2 and interacted with the quadrupolar CO_2 to improve CO_2 solubility, enhancing CO_2 permeability and selectivity.

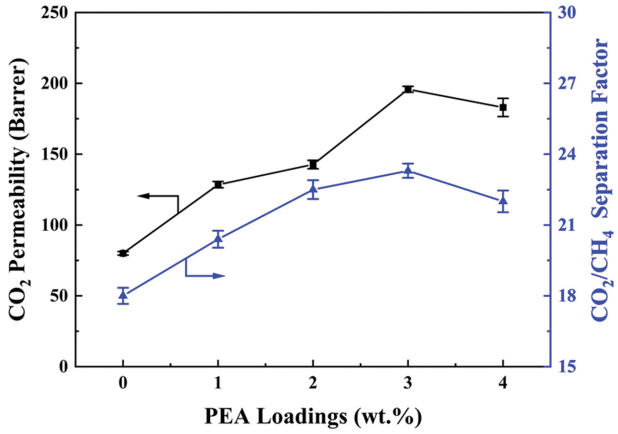

Fig. 10. CO_2/CH_4 separation performances of pure Pebax membrane and Pebax/PEA blend membranes under dry condition.

In addition, PEA containing PEO chains provides a microenvironment similar to that of the mobile carriers for amino groups, which allows CO_2 to be subjected to oscillating transport by amino groups while dissolving. Therefore, PEA contains amino groups that act as mobile carriers to tailor the chemical microenvironment in membranes. The mobile amino carriers preferentially react reversibly with CO_2 molecules, facilitating CO_2 transport in blend membranes [59-61]. Therefore, CO_2/CH_4 separation performance of blend membranes is greatly improved by introducing liquid-like PEA additive.

The main reason for the decrease in CO_2 separation performance of Pebax/PEA-4 blend membranes was the excessive PEA loadings, which will accumulate in membrane, resulting in a decrease in the number of revealable active sites. Nevertheless, CO_2/CH_4 separation performance of Pebax/PEA-4 blend membrane was still significantly improved in comparison with that of pure Pebax membrane.

2-2. Effect of Feed Pressure

The effect of feed pressure on CO_2 separation performance of Pebax/PEA-3 blend membrane with the optimal PEA loadings and pure Pebax membrane was investigated. The experimental results are indicated in Fig. 11. The feed pressure increased from 2 bar to 8 bar; both CO_2 permeability and CO_2/CH_4 separation factor of membranes showed a declining trend. The reason for the decrease in CO_2/CH_4 separation performance was as follows: As the feed pressure increased, the polymer chains became compact and the carrier saturation effect appeared [2,6,62].

CO_2 permeability and CO_2/CH_4 separation factor of pure Pebax membrane were reduced by 25% and 37.8%, respectively. However, CO_2 permeability and CO_2/CH_4 separation factor of Pebax/PEA-3 blend membrane was reduced by 18.3% and 22.7%, respectively. The decrease in CO_2 separation performance of Pebax/PEA-3 blend membrane was lower than that for pure Pebax membrane. This is mainly attributed to the introduced PEA, which can promote CO_2 separation performance of blend membranes at a high feed pressure. In addition, CO_2 solubility in PEA increased with increasing feed pressure, which implied that the introduced PEA enhanced separation performance of Pebax/PEA-3 blend membrane and over-

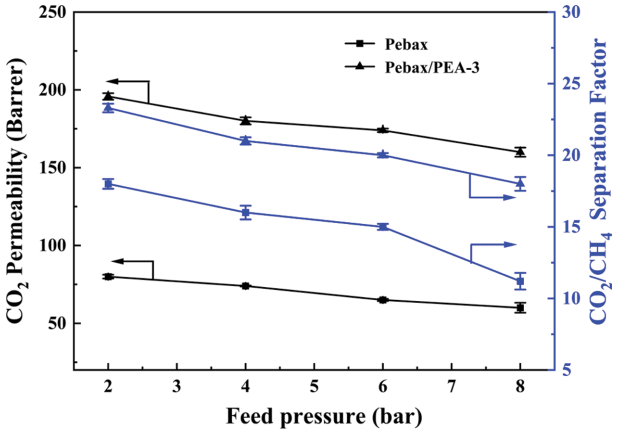

Fig. 11. Effect of feed pressure on CO_2/CH_4 separation performance of pure Pebax membrane and Pebax/PEA blend membranes under dry condition.

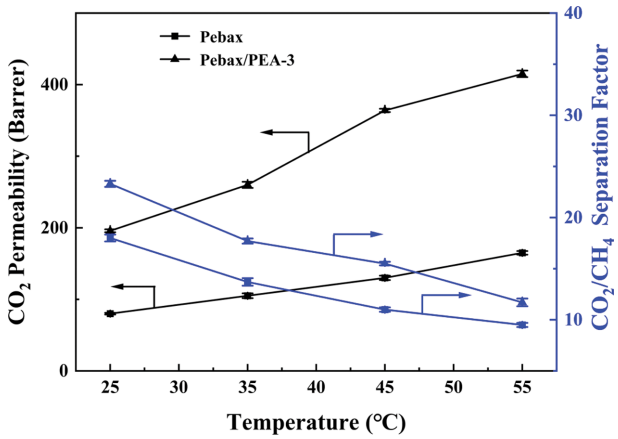

Fig. 12. Effect of operating temperature on CO_2/CH_4 separation performance of pure Pebax membrane and Pebax/PEA blend membranes under dry condition.

came the negative effects of a high feed pressure.

2-3. Effect of Operating Temperature

The effect of operating temperature on CO_2 separation performance of Pebax/PEA-3 blend membrane with optimal PEA loadings and pure Pebax membrane was investigated. The experimental results are shown in Fig. 12. It can be clearly observed that CO_2 permeability and CO_2/CH_4 separation factor of membranes increased and decreased, respectively, with increasing operating temperature. The operating temperature was increased from 25 °C to 55 °C, the mobility of the polymer chains was increased, resulting in an increase in gas diffusivity and a decrease in gas separation factor. Furthermore, Pebax/PEA-3 blend membrane had a higher CO_2/CH_4 separation performance than that of pure Pebax membrane. This was mainly attributed to the introduced PEA, which improved CO_2/CH_4 separation performance.

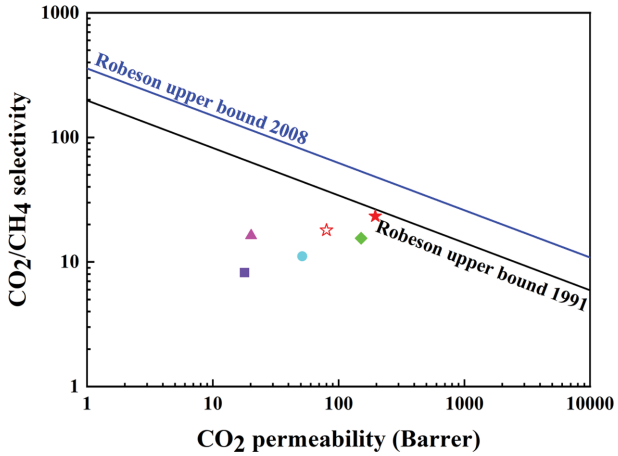

Fig. 13. Comparison of CO_2/CH_4 separation performance between this work and other studies in comparison with the Robeson upper bound: (☆) Pure Pebax (this work), (★) Pebax/PEA-3 (this work), (▲) PVC/PVIm, (■) PILPyr-TFSI/P(VBCImTFSI-co-AA20), (◆) Pebax/PEG-200, and (●) Pebax/NaCl.

3. Comparison with Blend Membranes of Other Works

In this work, Fig. 13 exhibits CO_2/CH_4 separation performance of pure Pebax membrane and Pebax/PEA-3 blend membrane in comparison with that of other blend membranes by the Robeson upper bound [24,29,36,63]. Fig. 13 shows that CO_2/CH_4 separation performance of Pebax/PEA-3 blend membrane was significantly improved by introducing liquid-like PEA additive and was better than that of some blend membranes. This highlighted that liquid-like PEA was a promising additive for CO_2 separation. In addition, CO_2 separation performance of the blended material was superior to that of the single material. This implies that PEA played a vital role in improving CO_2 separation performance of blend membranes.

CONCLUSION

Pebax/PEA blend membranes were systematically fabricated for CO_2/CH_4 separation. The results indicated that CO_2 separation performance of Pebax/PEA blend membranes was significantly improved with the introduction of PEA. The CO_2 permeability and CO_2/CH_4 separation factor of the optimal Pebax/PEA-3 blend membrane were 195.8±2.1 barrer and 23.3±0.3, increasing by 144.8% and 29.4% in comparison with pure Pebax membrane, respectively. The increased CO_2/CH_4 separation performance was mainly attributed to the introduced PEA, which tailored the physical and chemical microenvironments in blend membranes. On one hand, the introduced PEA was a liquid-like additive, which can tailor the physical microenvironment in Pebax/PEA blend membrane to reduce the transfer resistance of gases. On the other hand, PEA contained amino mobile carriers, which preferentially reacted reversibly with CO_2 molecules, facilitating CO_2 transport in blend membranes. This implied that the PEA acted as a mobile carrier to tailor the chemical microenvironment in blend membranes, which enhanced gas permselectivity. Therefore, the introduction of PEA is a novel strategy for tailoring the physical and chemical microenvironments in blend membranes for efficient CO_2/CH_4 separation.

ACKNOWLEDGEMENTS

This work was supported by the National Natural Science Foundation for Young Scientists of China [grant number 21706166]; Program for Young and Middle-aged Scientific and Technological Innovation Leaders in Bingtuan [grant number 2019CB024]; the Program for Young Innovative Talents of Shihezi University [grant numbers CXRC201802, CXRC201704]; and the Major Science and Technology Project of Xinjiang Bingtuan [grant number 2017AA007/01]; the National Natural Science Foundation of China [grant number 21661027]; and the Research and innovation projects for Postgraduates in Xinjiang Autonomous Region [grant number XJ2021G106]. We wish to thank the Analysis and Testing Center of Shihezi University for the microscopy and microanalysis of our specimens.

SUPPORTING INFORMATION

Additional information as noted in the text. This information is

available via the Internet at http://www.springer.com/chemistry/journal/11814.

REFERENCES

1. X. Li, J. Hou, R. Guo, Z. Wang and J. Zhang, *ACS Appl. Mater. Inter.*, **11**, 24618 (2019).
2. S. Ding, X. Li, S. Ding, W. Zhang, R. Guo and J. Zhang, *Sep. Purif. Technol.*, **239**, 116539 (2020).
3. M. A. O. Lourenço, C. Nunes, J. R. B. Gomes, J. Pires, M. L. Pinto and P. Ferreira, *Chem. Eng. J.*, **362**, 364 (2019).
4. M. Mozafari, R. Abedini and A. Rahimpour, *J. Mater. Chem. A.*, **6**, 12380 (2018).
5. M. Z. Ahmad, T. A. Peters, N. M. Konnertz, T. Visser, C. Téllez, J. Coronas, V. Fila, W. M. de Vos and N. E. Benes. *Sep. Purif. Technol.*, **230**, 115858 (2020).
6. J. Zhang, Q. Xin, X. Li, M. Yun, R. Xu, S. Wang, Y. Li, L. Lin, X. Ding, H. Ye and Y. Zhang, *J. Membr. Sci.*, **570-571**, 343 (2019).
7. S. M. A. Ahmadi, T. Mohammadi and N. Azizi, *Korean J. Chem. Eng.*, **38**, 104 (2021).
8. G. Yu, Y. Li, Z. Wang, T. X. Liu, G. Zhu and X. Zou, *J. Membr. Sci.*, **591**, 117343 (2019).
9. H. Kweon, C.-W. Lin, M. M. Faruque Hasan, R. Kaner and G. N. Sant, *ACS Appl. Polym. Mater.*, **1**, 3233 (2019).
10. C. Altintas and S. Keskin, *ACS Sustain. Chem. Eng.*, **7**, 2739 (2019).
11. Y. Wu, T. Zhou, H. Wu, W. Fu, X. Wang, S. Wang, L. Yang, X. Wu, Y. Ren, Z. Jiang and B. Wang, *J. Membr. Sci.*, **563**, 229 (2018).
12. X. Zou and G. Zhu, *Adv. Mater.*, **30**, 1700750 (2018).
13. T. Zhang, J. Yin, Y. Pan, E. Liu, D. Liu and J. Meng, *Chem. Eng. J.*, **383**, 123166 (2020).
14. K. Xie, Q. Fu, G. G. Qiao and P. A. Webley, *J. Membr. Sci.*, **572**, 38 (2019).
15. X. Li, S. Ding, J. Zhang and Z. Wei, *Int. J. Greenh. Gas Con.*, **101**, 103136 (2020).
16. T. Yan, Y. Lan, M. Tong and C. Zhong, *ACS Sustain. Chem. Eng.*, **7**, 1220 (2018).
17. R. L. Thankamony, X. Li, S. K. Das, M. M. Ostwal and Z. Lai, *J. Membr. Sci.*, **591**, 117348 (2019).
18. H. Sanaeepur, R. Ahmadi, A. E. Amooghin and D. Ghanbari, *J. Membr. Sci.*, **573**, 234 (2019).
19. M. Raouf, R. Abedini, M. Omidkhah and E. Nezhadmoghadam, *Process Saf. Environ.*, **133**, 394 (2020).
20. S. Meshkat, S. Kaliaguine and D. Rodrigue, *Sep. Purif. Technol.*, **212**, 901 (2019).
21. B. N. Gacal, V. Filiz and V. Abetz, *Macromol. Chem. Phys.*, **217**, 672 (2016).
22. L. Huang, J. Liu and H. Lin, *J. Membr. Sci.*, **610**, 118253 (2020).
23. C. Yi, Z. Wang, M. Li, J. Wang and S. Wang, *Desalination*, **193**, 90 (2006).
24. W. Fam, J. Mansouri, H. Li, J. Hou and V. Chen, *Ind. Eng. Chem. Res.*, **58**, 3304 (2019).
25. S. Mazinani, R. Ramezani, S. Darvishmanesh, G. F. Molelekwa, R. Di Felice and B. Van der Bruggen, *J. CO_2 Util.*, **27**, 536 (2018).
26. I. Hossain, A. Z. Al Munsur, O. Choi and T.-H. Kim, *Sep. Purif. Technol.*, **224**, 180 (2019).
27. M. R. Dilshad, A. Islam, U. Hamidullah, F. Jamshaid, A. Ahmad, M. T. Z. Butt and A. Ijaz, *Sep. Purif. Technol.*, **210**, 627 (2019).
28. Z. Dai, J. Deng, L. Ansaloni, S. Janakiram and L. Deng, *J. Membr. Sci.*, **578**, 61 (2019).
29. T. Chouliaras, A. Vollas, T. Ioannides, V. Deimede and J. Kallitsis, *Membranes*, **9**, 164 (2019).
30. S. Abdollahi, H. R. Mortaheb, A. Ghadimi and M. Esmaeili, *J. Membr. Sci.*, **557**, 38 (2018).
31. M. S. Suleman, K. K. Lau and Y. F. Yeong, *J. Nat. Gas. Sci. Eng.*, **52**, 390 (2018).
32. J. Deng, Z. Dai, J. Yan, M. Sandru, E. Sandru, R. J. Spontak and L. Deng, *J. Membr. Sci.*, **570-571**, 455 (2019).
33. R. Castro-Muñoz, V. Fíla, V. Martin-Gil and C. Muller, *Sep. Purif. Technol.*, **210**, 553 (2019).
34. H. Zhang, H. Tian, J. Zhang, R. Guo and X. Li, *Int. J. Greenh. Gas Con.*, **78**, 85 (2018).
35. S. Feng, J. Ren, D. Zhao, H. Li, K. Hua, X. Li and M. Deng, *J. Energy Chem.*, **28**, 39 (2017).
36. A. Car, C. Stropnik, W. Yave and K.-V. Peinemann, *J. Membr. Sci.*, **307**, 88 (2008).
37. S. R. Reijerkerk, M. H. Knoef, K. Nijmeijer and M. Wessling, *J. Membr. Sci.*, **352**, 126 (2010).
38. X. Wang, W. Zeng, M. Song, F. Wang, X. Hu, Q. Guo and Y. Liu, *Chem. Eng. J.*, **364**, 475 (2019).
39. A. A. M. Salih, C. Yi, H. Peng, B. Yang, L. Yin and W. Wang, *J. Membr. Sci.*, **472**, 110 (2014).
40. D. Wang, S. Song, W. Zhang, Z. He, Y. Wang, Y. Zheng, D. Yao, Y. Pan, Z. Yang, Z. Meng and Y. Li, *Sep. Purif. Technol.*, **241**, 116708 (2020).
41. J. Wang, W. Fang, J. Luo, M. Gao, Y. Wan, S. Zhang, X. Zhang and A.-H. A. Park, *J. Membr. Sci.*, **584**, 79 (2019).
42. X. Fu, X. Li, R. Guo, J. Zhang and X. Cao, *High Performance Polymers*, **30**, 1064 (2017).
43. X. You, J. Zhang, L. Shen, R. Li, Y. Xu, M. Zhang, H. Hong, L. Yang, Y. Ma and H. Lin, *J. Membr. Sci.*, **635**, 119532 (2021).
44. J. Wu, M. Xia, Z. Li, L. Shen, R. Li, M. Zhang, Y. Jiao, Y. Xu and H. Lin, *J. Membr. Sci.*, **638**, 119699 (2021).
45. Y. Long, G. Yu, L. Dong, Y. Xu, H. Lin, Y. Deng, X. You, L. Yang and B.-Q. Liao, *Water Res.*, **189**, 116665 (2021).
46. R. Li, L. Rao, J. Zhang, L. Shen, Y. Xu, X. You, B.-Q. Liao and H. Lin, *J. Membr. Sci.*, **635**, 119502 (2021).
47. M. Liu, M. D. Nothling, P. A. Webley, J. Jin, Q. Fu and G. G. Qiao, *Chem. Eng. J.*, **396**, 125328 (2020).
48. X. Lv, L. Huang, S. Ding, J. Wang, L. Li, C. Liang and X. Li, *Sep. Purif. Technol.*, **276**, 119347 (2021).
49. H. Lin and B. D. Freeman, *J. Membr. Sci.*, **239**, 105 (2004).
50. L. Sheng, Y. Guo, D. Zhao, J. Ren, S. Wang and M. Deng, *J. Nat. Gas. Sci. Eng.*, **75**, 103123 (2020).
51. Y. Liu, H. Wu, S. Wu, S. Song, Z. Guo, Y. Ren, R. Zhao, L. Yang, Y. Wu and Z. Jiang, *J. Membr. Sci.*, **618**, 118693 (2021).
52. F. Li, C. Zhang and Y. Weng, *Macromol. Chem. Phys.*, **220**, 1900047 (2019).
53. S. Wang, Y. Liu, S. Huang, H. Wu, Y. Li, Z. Tian and Z. Jiang, *J. Membr. Sci.*, **460**, 62 (2014).
54. B. Sasikumar, S. Bisht, G. Arthanareeswaran, A. F. Ismail and M. H. D. Othman, *Sep. Purif. Technol.*, **264**, 118471 (2021).
55. N. Zhang, H. Wu, F. Li, S. Dong, L. Yang, Y. Ren, Y. Wu, X. Wu, Z.

Jiang and X. Cao, *J. Membr. Sci.*, **567**, 272 (2018).
56. X. Wu, Z. Tian, S. Wang, D. Peng, L. Yang, Y. Wu, Q. Xin, H. Wu and Z. Jiang, *J. Membr. Sci.*, **528**, 273 (2017).
57. C. Soto, C. Aguilar Lugo, S. Rodríguez, L. Palacio, Á. E. Lozano, P. Prádanos and A. Hernandez, *Sep. Purif. Technol.*, **247**, 116895 (2020).
58. Y. Yampolskii, *Macromolecules*, **45**, 3298 (2012).
59. X. Cao, Z. Wang, Z. Qiao, S. Zhao and J. Wang, *ACS Appl. Mater. Inter.*, **11**, 5306 (2019).
60. J. Liao, Z. Wang, C. Gao, S. Li, Z. Qiao, M. Wang, S. Zhao, X. Xie, J. Wang and S. Wang, *Chem. Sci.*, **5**, 2843 (2014).
61. J. Liao, Z. Wang, C. Gao, M. Wang, K. Yan, X. Xie, S. Zhao, J. Wang and S. Wang, *J. Mater. Chem. A.*, **3**, 16746 (2015).
62. H. Rajati, A. H. Navarchian, D. Rodrigue and S. Tangestaninejad, *Sep. Purif. Technol.*, **235**, 116149 (2020).
63. N. Noorani and A. Mehrdad, *J. Mol. Liq.*, **292**, 111410 (2019).

Supporting Information

Tailoring physical and chemical microenvironments by polyether-amine in blended membranes for efficient CO_2 separation

Xia Lv*, Xueqin Li*,†, Lu Huang*, Siyuan Ding*, Yin Lv*, and Jinli Zhang*,,†**

*School of Chemistry and Chemical Engineering/Key Laboratory for Green Processing of Chemical Engineering of Xinjiang Bingtuan, Shihezi University, Shihezi, Xinjiang, 832003, China
**Key Laboratory for Green Chemical Technology of Ministry of Education, School of Chemical Engineering and Technology, Tianjin University, Tianjin 300072, China
(*Received 19 June 2021 • Revised 19 October 2021 • Accepted 20 October 2021*)

S1. The Self-built Permeation Measurement Equipment

Fig. S1. The real picture of the self-built permeation measurement equipment for gas permeation.

S2. Pictures of Contact Angle From the Camera

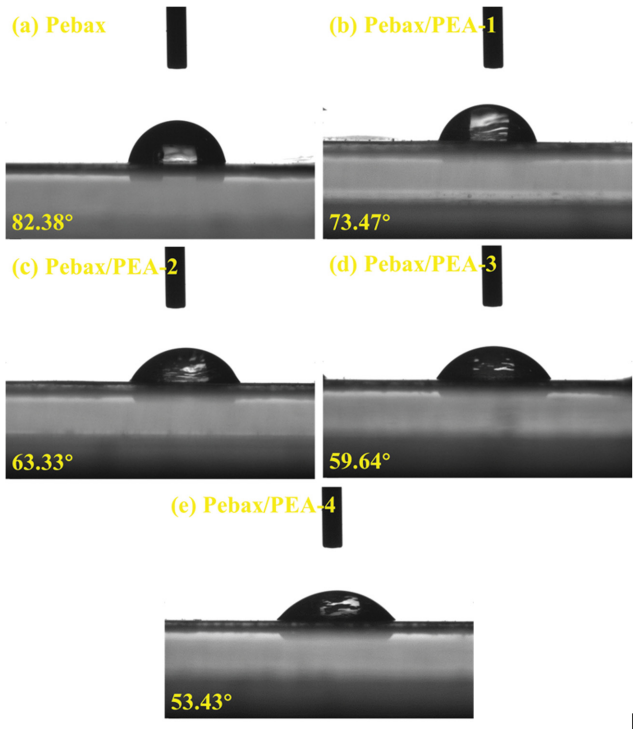

Fig. S2. The pictures of real contact angle of the membranes from the camera: (a) Pebax, (b)-(e) Pebax/PEA blend membranes.